SAKARYA UNIVERSITY JOURNAL OF COMPUTER AND INFORMATION SCIENCES
http://saucis.sakarya.edu.tr/
e-ISSN: 2636-8129
Publisher: Sakarya University
Vol. 8, No. 2, 184-197, 2025
DOI: 10.35377/saucis..1665478
RESEARCH ARTICLE

LungDxNet: AI-Powered Low-Dose CT Analysis for Early Lung Cancer Detection

Premananda Sahu[1], Ashwani Kumar[2], Mahesh Singh[3], Rituraj Jain[4], Kamal Upreti [5,*], Jyoti Parashar[6]

[1]Lovely Professional University, School of CSE, Jalandhar, Punjab, India, ror.org/00et6q107
[2]Bennett University, School of Computer Science Engineering & Technology, Greater Noida, UP India, ror.org/00an5hx75
[3]Aditya University, Department of ECE, Surampalem, India, ror.org/03pztks36
[4]Marwadi University, Department of Information Technology, Rajkot, Gujarat, India, ror.org/030dn1812
[5]Christ University, Department of Computer Science, Delhi NCR Campus, Ghaziabad, India, ror.org/022tv9y30
[6]Bharati Vidyapeeth's Institute of Computer Applications & Management, Department of Computer Application, Delhi, India

Corresponding author:
Kamal Upreti, School of Sciences, Department of Computer Science, Christ University, Delhi NCR Campus, Ghaziabad, India
kamalupreti1989@gmail.com

Article History:
Received: 25.03.2025
Revised: 20.04.2025
Accepted: 21.04.2025
Published Online: 13.06.2025

ABSTRACT

Early and accurate diagnosis, however, is still lacking for the most common form of lung cancer, and this remains one of the leading cancers leading to mortality. CT scans are widely used for lung cancer screening; however, their manual interpretation is time-consuming and prone to variability. This study introduces LungDxNet, a deep learning-based framework that integrates transfer learning to enhance diagnostic accuracy and efficiency. Using a large dataset of Low Dose CT (LDCT) scans, the system is built with fine-tuned pre-trained Convolutional Neural Networks (CNNs) such that feature extraction is reliable though minimal reducing radiation exposure. Consequently, LungDxNet involves the integration of component segmentation techniques that have been used to isolate the lung regions and discriminate the cancerous nodules from the malignant and benign cases. Very rigorous evaluations were performed on the model against both conventional machine learning and state of the art deep learning architectures. Results show that there is a substantial reduction of false positive and false negative resulting in a superior accuracy (98.88), sensitivity, and specificity. This design is to be scaled, robust and clinically applicable, making it a potential real world lung cancer diagnosis tool. Deep learning and transfer learning has excellent power to transform lung cancer detection, and this research brings awareness of how far we can optimise and integrate into clinical workflow. The model is enhanced for future work and adapted for real time diagnostic applications.

Keywords: Lung Cancer, Deep Learning, Machine Learning, Low Dose CT, Artificial Intelligence

1. Introduction

Lung cancer is a significant health issue and remains the primary cause of a large proportion of deaths that occur with this illness. Concerning survival, identification is among the most excellent tools because early interventions may even change the course of the disease. It is generally agreed that CT scan visioning is the best technique for lung deviations; however, there are some time-consuming with subjectively dependent manual diagnoses by radiologists. It reflects the requirement for automatic, fixed, and scalable resolutions for clinical experts as they proceed to perform their investigative activities. AI has been introduced in medicinal visioning and is proving divergent for many different domains. Deep learning, which automatically learns features from large complex datasets by generalization, has caught much attention in the current AI community. Among the CNNs belonging to the more prominent family of DL, they are capable of impressive performance on image categorization and decomposition tasks [1].

On the other hand, the system needs large amounts of explained data to train from scratch, and in much relevance, including medical, such annotated datasets are complex to come by. Transfer learning is one of the most potent strategies against these challenges above. Transfer learning assists in making use of pre-trained models, which have cultured the general aspects of gigantic data like ImageNet. Fine-tuning such models on context-specified data enables the attainment of elevated accomplishment with significantly much smaller datasets.

This research explores the possibility of utilizing DL coupled with transfer learning in the creation of a self-regulated lung cancer recognition system. The idea to be introduced here is fine-tuning pre-trained CNNs towards classifying lung low-dose

Cite as: P. Sahu, A. Kumar, M. Singh, R. Jain, K. Upreti, and J. Parashar. (2025). Lungdxnet: Ai-powered low-dose ct analysis for early lung cancer detection. *Sakarya University Journal of Computer and Information Sciences*. vol. 8, no. 2, pp. 184-197, 2025 doi: 10.35377/saucis...1665478

This work is licensed under Creative Commons Attribution-NonCommercial 4.0 International License

CT scans into cancerous and non-cancerous cases. The identification of lung cancer using deep learning relies on several key techniques to enhance accuracy and robustness. The process begins with lung region segmentation, which isolates the lung area from medical images, removing irrelevant background structures. This supports the fact that the model concentrates only on lung tissues and rises within feature extraction. Then, data augmentation deals with the problem of class imbalance by artificially growing the diversity of training instances. In this, techniques like rotation, flipping, and contrast adjustments create variations of lung images, so the model is not geared toward dominant classes, and its ability to generalize, among other cases, improves. For feature extraction, VGGNet, ResNet, and InceptionNet are used in advanced deep learning architecture. The patterns captured by these networks are very complex in medical images. However, given the deep convolutional layers of VGGNet, hierarchical features are extracted. ResNet, utilizing residual connections, ensures deeper network training without vanishing gradients, making it highly effective for complex image analysis [2]. InceptionNet, with its multi-scale feature extraction, captures fine details and structural variations in lung nodules, which is essential for differentiating between benign and malignant cases. The main aim would be to produce effective, automatically enhanced clinical workflows, thereby avoiding potential diagnostic errors and accelerating efforts made towards its detection from the earliest stages.

1.1.Motivation

Though medical imaging has seen numerous improvements, conventional methods of lung cancer diagnosis particularly those reliant on manual CT scan assessment are still largely encumbered by subjectivity, time consumption, and inter-observer variability. These constraints create serious problems in the early detection of lung cancer, where a successful diagnosis can make a difference between living and dying. Deep learning (DL) models have been shown to automate these tasks, but a lot depends on the availability of large, well-annotated datasets, which are very scarce in the medical field owing to privacy issues, labelling complexity, and expert dependency. In order to overcome these limitations, this study proposed a LungDxNet, a novel deep learning based deep learning framework that coalesces model fine tuning along with explainable AI on lung regions. This directly lowers the false positives/negatives on LungDxNet, improves model interpretability and allows the real time deployment in clinical settings while overcome from the gaps indicated in table 1.

The primary contributions of this work are as follows:

1. This study developed LungDxNet, an AI-driven system utilizing fine-tuned CNN models optimized for Low-Dose CT (LDCT) scan analysis to detect lung cancer at an early stage.
2. This study introduced a robust lung segmentation technique to isolate the lung region and enhance feature extraction, improving classification between malignant and benign nodules.
3. This study applied explainable AI techniques to improve model transparency and clinical trustworthiness.
4. This study extensively evaluated proposed model on a large LDCT dataset, demonstrating superior accuracy (98.88%) compared to traditional machine learning and recent deep learning approaches.
5. This study provides a scalable, real-time compatible solution that can be adapted for clinical lung cancer screening workflows.

This paper will be presented as follows: the review of the research gives a summary overview of the present methodologies used and highlights the areas this work seeks to bridge. Then, the methodology section extends with a presentation of the data processing pipeline, model architectures, and training strategy adopted in this work. Finally, results and discussions provide an in-depth analysis of the model's performance in relation to its clinical relevance and integration into the real-world setting.

2. Literature Review

Thus, low dose computed tomography (LDCT) has become a promising tool for early lung cancer detection with the potential to reduce mortalities [3]. Nevertheless, despite this, high false positive rates and dependence on the expertise of radiologists have limited its widespread adoption [4-6]. Artificial intelligence (AI) and machine learning (ML) techniques have integrated promise to overcome some of these challenges and improve lung cancer screening accuracy and efficiency [7-13].

AI could bring a lot to improving patient outcomes in lung cancer screening workflows [14]. With the help of AI-powered reconstruction techniques, less radiation can be given, and yet the image quality remains optimal, addressing concerns about the radiation exposure of CT scans [15]. One of the interesting uses of the application of AI algorithms, mainly deep learning (DL) models, has shown very high accuracy in the detection of lung nodules and classifies them as benign or malignant. For example, the accuracy of a 3x3 kernel convolutional neural network in lung nodule detection and classification was 97.56%, and the specificity was 98.4% [16].

Such integration of AI-driven analysis onto LDCT has multiple advantages compared to existing screening methods, including imaged and clinical data analysis and risk stratification. Computer-aided detection (CAD) systems have enhanced the automatic detection of potential lung nodules with high sensitivity and reduced the reading time for a concurrent or second reader. Furthermore, AI-based approaches facilitate the automatic segmentation and assessment of lesion size, volume, and

densitometric features, as well as radiomic feature extraction for comprehensive nodule characterisation [14].

At the same time that early-stage lung cancer detection has been increasingly popular using AI leveraging deep learning models, the use of such models for this purpose has become commonplace. P. Sathe et al. [17] used TNM (Tumor, Lymph Nodes, metastasis) classification to develop a fully automated solution for the screening of lung cancer with a performance of 96.4%. In the same vein, N. Gautam et al. [18] developed a hybrid model based on ResNet, DenseNet, and EfficientNet (LIDC-IDRI validation dataset), of which the model achieves 97.23% accuracy with 98.6% sensitivity and decreases false negatives.

Additionally, HA Ewaidat and YE Brag [19] used a CNN-based model, YOLOV5, to detect lung nodules in CT images. The model was trained on 280 annotated scans of the LIDC-IDRI dataset and achieved a mean average precision of 92.27%. PG Mikhael et al. introduced a deep learning-based lung cancer risk prediction model using LDCT imaging [20], and they achieved an AUC of 0.92 at one year, which expands on personalised screening.

Spatial Pyramid Pooling and 3D Convolution Deep Screener (Deep learning method) beat previous state-of-the-art algorithms [21] with the area under the curve (AUC) equal to 0.892. Another study introduced a Computer-Aided Detection (CADe) system utilising deep learning features and genetic algorithm optimisation, achieving a detection accuracy of 96.25%, sensitivity of 97.5%, and specificity of 95% [22]. Additionally, a 3D interpretable hierarchical semantic convolutional neural network (HSNet) demonstrated superior diagnostic performance in detecting various aspects of lung nodules, including malignancy [23].

In further studies, DL models were compared to radiologists. C. Jacobs et al. [24] compared 11 radiologists with high-performing deep learning systems on LDCT for lung cancer detection and found AUC values of 0.9 for deep learning and comparable to the radiologists. Y. Wang et al. [25] developed a radiomics-aided reinforcement learning model for early lung cancer analysis among serial LDCT scans with an AUC of 0.88, which is better than that of the model here.

Furthermore, A. Saha et al. [26] used three of the three transfer learning models to classify lung cancer-based lung cancer CT images using a multiclass (Categorisation) and achieved an accuracy of 91%. L. In LDCT imaging to detect lung nodules, Song et al. [27] used CapsNet as a feature extractor and integrated it with a 3D CNN, getting a detection rate of 95.19%. J. Shao et al. [28] performed the deep learning models' implementation across 12,360 people in screening by LDCT in China, which reached an accuracy of 86.96% in lung cancer risk assessment through using AI.

Additionally, the concept of transfer learning has been explored to improve lung cancer detection models. R. Anand et al. [29], VGG 16, and Inception V3 architecture were applied over the IQ _OThnccd lung cancer dataset, and their classification accuracy outcome was 96%. While this is, their study also showed key limitations: the necessity of a lot of labelled datasets, biases in the database, and capabilities to adapt pre-trained networks to medical problems.

Despite a great deal of progress in using AI to analyse LDCT, challenges exist. Refining AI models for lung cancer screening is necessary to mitigate high false positive rates. Furthermore, for healthcare centres, DL-based detection models are computationally demanding and present difficulties in implementing these technologies. In addition, radiologists' presence is essential to compensate for algorithmic bias and clinical validation and improve diagnostic accuracy [4].

Moving forward, it will be necessary to continue research and clinical validation of AI-powered LDCT analysis so that it can be brought into routine clinical practice. Gaps in data quality, algorithmic bias, and computational efficiency will have to be resolved in order to optimise AI for lung cancer screening. Collaboration between AI technology and human expertise could be the solution to refining the processes of lung cancer screening and improving patient outcomes [4, 30].

Additionally, the existing literature shows how much has been achieved in AI powered LDCT analysis for lung cancer detection early. Although deep learning models show notable progress, such as false positive and false negative rates, lack of dataset, being interpretable, and yet deploying in a real-time clinical environment, there remain still challenges. Addressing such gaps herein is described LungDxNet, a deep learning-based framework that incorporates transfer learning fine-tuned for pre-trained CNN architectures in enhanced diagnostic efficiency and accuracy. By leveraging advanced segmentation techniques, optimised feature extraction, and explainable AI methods, this research aims to bridge the identified gaps and provide a scalable, robust, and clinically applicable lung cancer detection solution. To systematically bridge the gaps identified in prior studies, this research formulates key research questions and addresses them through the proposed LungDxNet framework. Table 1 presents an overview of the significant research gaps, corresponding research questions, and how they are fulfilled in this study.

Having established the research gaps and their solutions, the following section details the methodology adopted to develop and evaluate the LungDxNet model, including data preprocessing, feature extraction, and classification techniques.

Table 1. Research Gaps, Corresponding Research Questions, and How They Are Addressed in This Study

Research Questions	Research Gaps	How These Questions Were Fulfilled
How can AI-powered lung cancer detection models be improved to minimise false-positive and false-negative rates?	High false-positive and false-negative rates in existing AI-powered lung cancer detection models.	LungDxNet utilises a fine-tuned CNN model and transfer learning to improve diagnostic accuracy, reducing false-positive and false-negative rates.
What strategies can be used to enhance the availability and quality of LDCT datasets for training deep learning models?	Limited availability of large, high-quality annotated LDCT datasets for deep learning model training.	The study leveraged a large LDCT dataset, applying augmentation techniques to enhance data quality and diversity.
How can AI algorithms be optimised to improve the differentiation between malignant and benign lung nodules?	Challenges in distinguishing between malignant and benign lung nodules with high accuracy.	A combination of segmentation techniques and deep learning-based classification improves differentiation between malignant and benign nodules.
What methodologies can facilitate the real-time deployment of AI-based lung cancer detection models in clinical settings?	Limited real-time deployment of AI-powered lung cancer detection models in clinical settings.	The model was designed with scalability and robustness in mind, enabling real-time diagnostic applications in clinical settings.
How can the interpretability and transparency of deep learning-based lung cancer detection models be enhanced?	Lack of interpretability and transparency in deep learning-based lung cancer detection models.	The study integrated explainable AI techniques to improve the transparency and interpretability of deep learning-based decisions.
What optimisations can be made to CNN-based feature extraction techniques to improve accuracy and efficiency?	Need for optimisation of CNN-based feature extraction techniques for better accuracy and efficiency.	Feature extraction was optimised using VGGNet, ResNet, and InceptionNet, ensuring improved accuracy y and efficiency.
How can AI models be effectively integrated with radiologists' expertise to enhance lung cancer diagnosis?	Challenges in integrating AI models with radiologists' expertise to enhance diagnostic performance.	The model's decision-making process was designed to work in conjunction with radiologists, enhancing human-AI collaboration.
What modifications can be made to deep learning models to improve their applicability in resource-constrained healthcare environments?	Limited adaptation of deep learning models for resource-constrained healthcare environments.	The proposed methodology reduces computational costs by using pre-trained models and optimising network architectures for efficiency.
How can the computational cost and processing time of deep learning-based lung cancer detection be minimised?	High computational costs and processing time are required for deep learning-based detection approaches.	By optimising network architectures and leveraging efficient training strategies, the computational demand and processing time were minimised.
What advancements in transfer learning can help enhance the performance of deep learning models trained on smaller datasets?	Need for improved transfer learning techniques to enhance the performance of deep learning models with smaller datasets.	Transfer learning techniques were fine-tuned, enabling the model to achieve high performance even with smaller datasets.

3. Methodology

This section consists of the proposed architecture in Fig.1, which describes the details of the model designed and the detailed steps expressed in a consequent manner:

1. A high-ranking medical radiologist usually conducts this test, and the input of microscopic cell images helps to detect and identify features of cancer in the primary phase.
2. The preprocessing phase describes discolouration and normalisation, which focus on the quality and consistency of the images. Noise Reduction eliminates artefacts and distortions unrelated to the actual contents of the image that may interfere with model performance, and normalisation equalises the pixel intensity values across images to ensure uniformity in the dataset.

3. Feature extraction, in this work, provides the procedure that employs deep convolutional neural networks (CNNs) to auto-extract important patterns and features present in the preprocessed images. The three well-established architectures are as follows:
    - VGGNet
    - ResNet
    - InceptionNet
4. The extracted features are fed into classification models to ascertain their likelihood of containing cancer. Three classifiers are attempted; these models map the deep features to specific classes primarily based on learned decision boundaries, and these are:
    - Fully Connected Neural Network (FCNN)
    - SoftMax Classifier
    - Support Vector Machine
5. Finally, the prediction result was produced in terms of normal, cancerous, and non-cancerous.

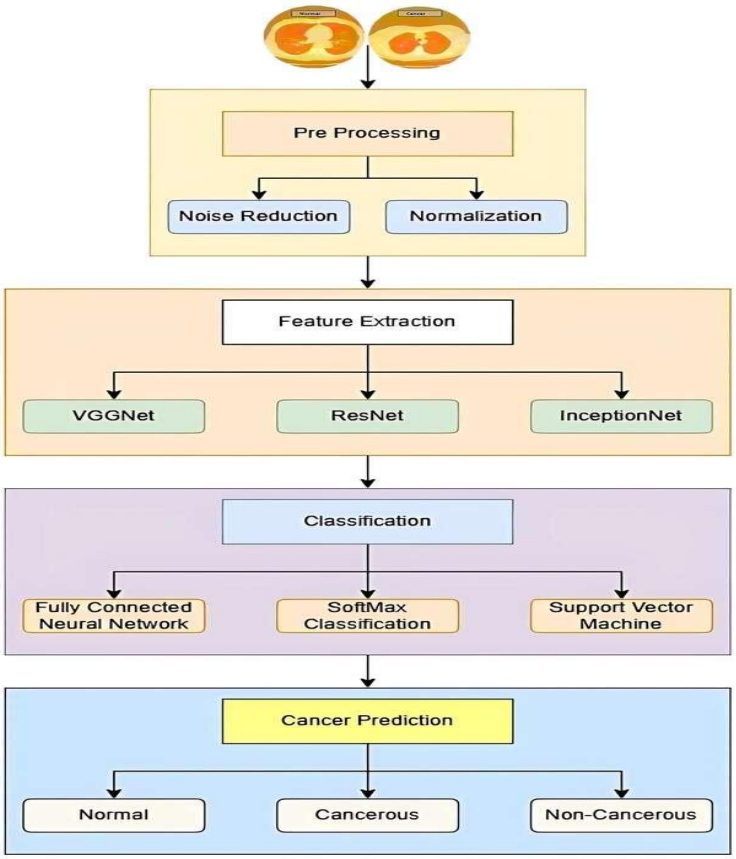

Figure 1: Complete architecture of the proposed LungDxNet framework for automatic classification of lung cancer using low-dose CT images.

3.1 Data Processing

The elimination of any disturbances and normalisation are crucial measures to progress picture excellence and model performance in the preprocessing stage of LDCT image lung cancer diagnosis. These types of images frequently cause significant levels of disturbances, which compromises image intelligibility. By regulating pixel concentration values throughout scans, normalisation improves the toughness of deep learning models. It has been done so that pixel values will be scaled onto a standard range; usually, it falls between 0 and 1 or -1 and 1, which makes the deep learning models better in terms of their convergence rate and performance. By focusing on important lung cancer attributes by means of noise lessening and normalisation, the deep learning model helps to improve nodule classification correctness and primary lung cancer diagnosis. Here, the Keras image data generator function was used.

3.2 Feature Extraction

Progressive CNN architecture is quite essential for feature removal from LDCT image-based lung cancer identification. Precise classification is made possible by these networks' instinctive learning of outlines and nodular traits at several intellectual levels. Here are some of the most predominantly utilised CNN architectures for feature removal and these are:

VGGNet (Visual Geometry Group Network)-: Applies several convolutional layers with insignificant kernel size, i.e. 3x3. Beginning from boundaries and surfaces, it hierarchically removes features till increasingly intricate lung cancer outlines. The innovative layers of VGGNet for identifying spiculated boundaries and compactness disparities play a critical role in distinguishing between normal, cancerous, and non-cancerous lungs.

ResNet—To address the issue of vanishing gradients in deep CNNs, ResNet (Residual Network) introduces skip connections, which allow for bypassing certain layers. These connections help information flow within the network without loss, ensuring that fine-grained lung nodule characteristics are well captured. Such improvement is due to Resnet's ability to extract texture, shape irregularities, and changes of contrast.

InceptionNet-: To obtain features at different scales at once, InceptionNet employs parallel convolutional layers with varying kernel sizes (1×1, 3×3, 5×5). This multi-scale approach enables the network to recognise nodules of differing sizes and densities in the LDCT images. These multi-scale approaches guarantee that both small isolated nodules and larger irregular tumours are well-defined, ensuring that all cases are effectively classified [31].

By mixing the above processes, the model proficiently learns discriminatory lung cancer-related data features, which are important to initial and precise lung cancer identification from LDCT images.

3.3 Classification

Fully Connected Neural Network (FCNN): An FCNN has individual neurons in a layer associated with each neuron in the subsequent layer. This way, a dense network of interconnections is formed. This architecture, therefore, allows the network to acquire complex patterns and relations within the data through the operation of weights throughout the training process [32]. Moreover, it shows excessive promise in supervised learning contexts such as image organisation, text classification, or in any submission where the goal is to allocate input data into one amongst a list of predefined groups. It comprises 3 main types, i.e. input, hidden and output layer.

The input layer gathers unprocessed fresh data. Every neuron in this layer relates to an input characteristic. For example, in image classification, the input may be a compressed vector of picture element strengths.

Hidden layers learn hierarchical, class-specific structures from LDCT data: The initial layers of the network learn to identify basic characteristics, including edges and textures, as well as noise patterns within low-dose medical images. The deeper layers integrate these basic features to form complex representations that capture details like nodule information. Now, the non-linear activation function ReLU enables the network to capture the lung nodules, which can be expressed as:

$$f(x)=\max(0,x) \tag{1}$$

Where f is a function, x is the input variable, and max returns the maximum value.

The output layer comprises a single neuron for each class, and the Softmax activation function translates the grooves into regularised probabilities.

For training FCNN, LDCT images with corresponding ground truth labels utilising the cross-entropy function that calculates loss function and are expressed as:

$$L = -\frac{1}{S}\sum_{j=1}^{S}\sum_{c=1}^{C} x_{j,c}\log\left(\hat{x}_{j,c}\right) \tag{2}$$

Where L is the loss function, S is the total number of samples, x_j,c is the ground truth for specified input with j sample, and class c and xˆis predicted probability.

Softmax Classifier: Let's familiarise the softmax classifier collected formerly to precisely classify lung conditions from a low-dose CT (LDCT) dataset into three classes: We will inspect how the classifier scrutinises LDCT data to dispersed normal conditions from cancerous and non-cancerous cases for lung cancer screening submissions. The softmax function stimulates the output layer to produce probability distributions over all three classes. The classification result is made by selecting the class that displays the highest probability [34]. The softmax function normalises output layer scores into probabilities during classification tasks. The FCNN establishes the neural network structure while the softmax function generates the output probabilities in this common combination. It is expressed as:

$$\text{Softmax}\,(q_c) = \frac{e^{q_c}}{\sum_k e^{q_k}} \tag{3}$$

Where q_c is the input score for class c, and k is another class.

The interior neural network framework of FCNN, where the relationship among laers is fully associated, is depicted in Fig.2.

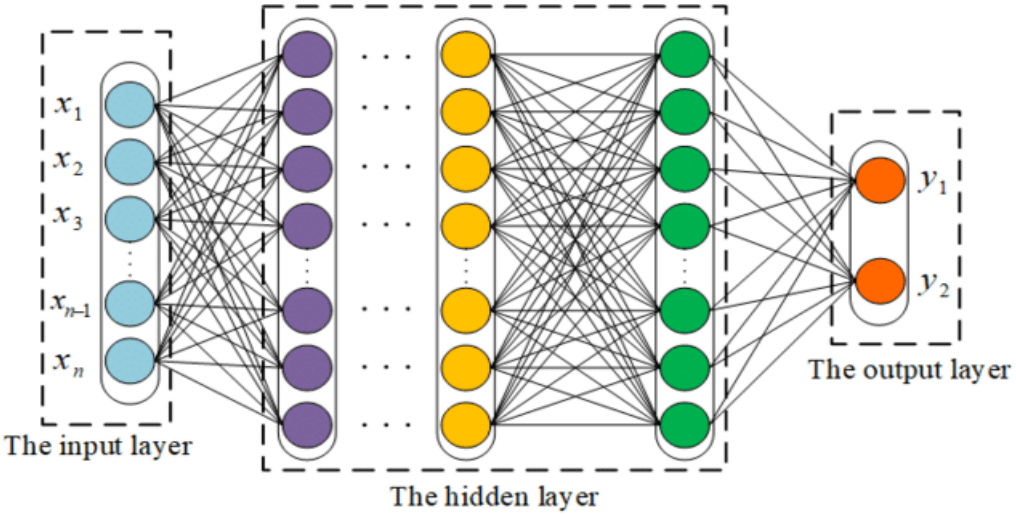

Figure 2: Architecture of the Fully Connected Neural Network (FCNN) model used for feature-based lung cancer classification in LDCT images [33]

Fig. 3 depicts the detailed softmax transformation and the FCNN pipeline for the visual flowchart.

Support Vector Machine: The system demonstrates proficiency in classification tasks by identifying the best boundary to divide distinct class data points within high-dimensional environments. In lung cancer detection, SVM uses LDCT image-derived features to accurately classify lung conditions as normal, cancerous, or non-cancerous. While neural networks train classified attributes, SVM influences predefined attributes and accomplishes well with a lesser dataset [35].

For the novel LDCT sample x, every SVM calculates the decision function expressed as:

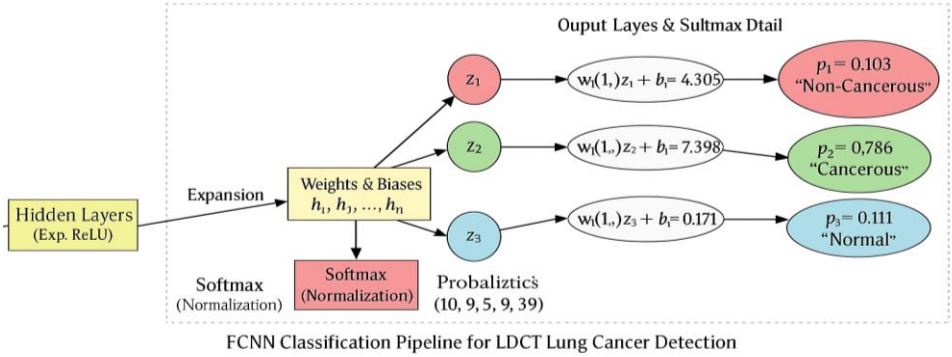

Figure 3: Complete architecture of the Fully Connected Neural Network (FCNN) pipeline used for Categorizing LDCT Lung Images into 3 Dissimilar Groups: Cancerous, Non-Cancerous, and Normal

$$f_c(x) = \sum_{j \in SV} m_j\, y_j\, k(x_j, x) + b \qquad (4)$$

Where fc (x) is the decision function with c as class and x is input, x_j is the support vector, m_j is the Lagrange multiplier with j^{th} support vector, y_j is the actual output, k is the kernel function, and b is bias.

The SVM decision-making process clearly classifies the above 3 classes based on the visual flowchart depicted in Fig.4.

It simplifies the classification of lung cancer in LDCT examinations by projecting image characteristics into an exalted dimensional space, identifying optimal hyperplanes to discriminate between normal, cancerous, and non-cancerous groups. Its benefit is in dealing with the noise inherent to LDCT and proficiently handling minor datasets, providing a dependable and explainable option associated with neural networks for the above groups.

LDCT and proficiently handling minor datasets, providing a dependable and explainable option associated with neural networks for the above groups.

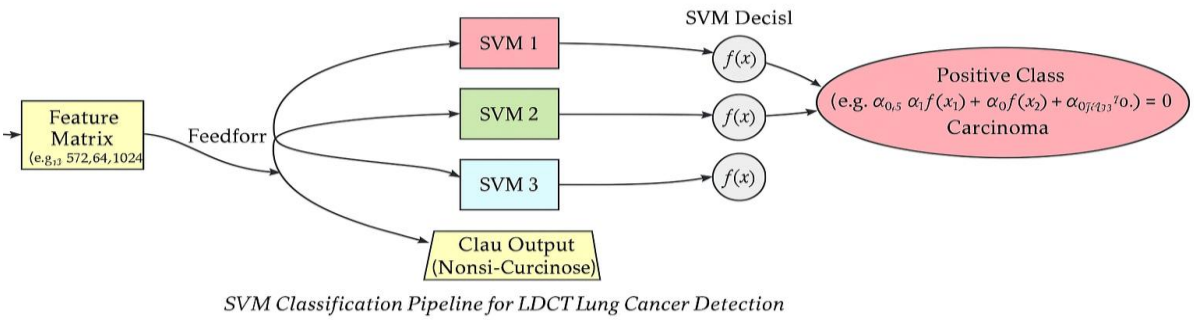

Figure 4: Support Vector Machine (SVM) pipeline for multi-class classification of lung cancer in LDCT images.

4. Result and Discussion

This section represents the implementation steps for the complete methodology for lung cancer classification, which is described below. The projected model for lung cancer classification was employed on a computer running Windows 11 OS, 64 bits as processing speed with 16GB of RAM, Google col-ab with tensor flow, and the Keras library.

4.1 Dataset

The detailed image dataset utilised to classify lung cancer using LDCT, i.e. Low Dose Computed Tomography and Projection dataset, are provided in this section [36]. By using existing lung cancer statistics and LDCT broadcast trends tailored to the Indian background. Indian lung cancer occurrence data and broadcast studies will learn these percentages. The total dataset contains 5378 LDCT images. The first class consists of non-cancerous lung cancer images (13%), comprising 592 scanned images. The second class includes 2661 cancerous lung cancer images (49%). The third class contains 2231 normal lung images (40%), all with dimensions of 512x512 pixels. In this study, 70% of the data is used for training, 20% for testing, and 10% for validation.

The assessment is done on the basis of performance matrices such as accuracy, precision, recall and f1 score. Accuracy is the description of accurately classified instances out of all cases. Recall measures the true positive occurrences classified out of actual positive occurrences [37]. Precision measures the true positive instances out of all positive instances, and they are expressed as:

$$\text{Accuracy} = \frac{\text{TP+TN}}{\text{TP+TN+FP+FN}} \quad (5)$$

$$\text{Precision} = \frac{\text{TP}}{\text{TP+FP}} \quad (6)$$

$$\text{Recall} = \frac{\text{TP}}{\text{TP+FN}} \quad (7)$$

After training from algorithms like FCNN, SoftMax classifier, and SVM, the model's training accuracy and loss, along with its validation accuracy and loss, have been determined. The performance metrics table for the above model is depicted in Table 2.

$$\text{F1 Score} = \frac{2*\text{Precision}*\text{Recall}}{\text{Precision+Recall}} \quad (8)$$

Table 2. Accomplishment Metrices for Individual Models

Model	Accuracy (%)	Precision (%)	Recall (%)	F1 Score (%)
SVM	94.54	93.52	93.85	94.01
SoftMax Classifier	97.42	96.86	97.03	96.78
FCNN	**98.88**	**97.84**	**98.81**	**97.62**

The above graphical presentation and table clearly compare each other, and the results are clearly achieved. Here, the authors categorised the images into normal, cancerous, and non-cancerous, and after training, the sample image is expressed in Fig.5. The following diagram shows examples of low-dose computed tomography scans serving as screening modalities in which

both positive (likely malignant) and negative (likely benign or normal) cases are observed. Each case must include a series of axial LDCT slices, all with regions of interest highlighted and the malignancy probability score corresponding. Each row contains multiple CT slices of the same case to portray the 3D perspective of either lesion or normal anatomy. All suspicious areas are marked with red circles, while white boxes identify the region analyzed for the possibility of malignancy.

Various performance metrics for the above 3 models are described separately in Table 3, and the corresponding ROC plot is illustrated in Fig.6.

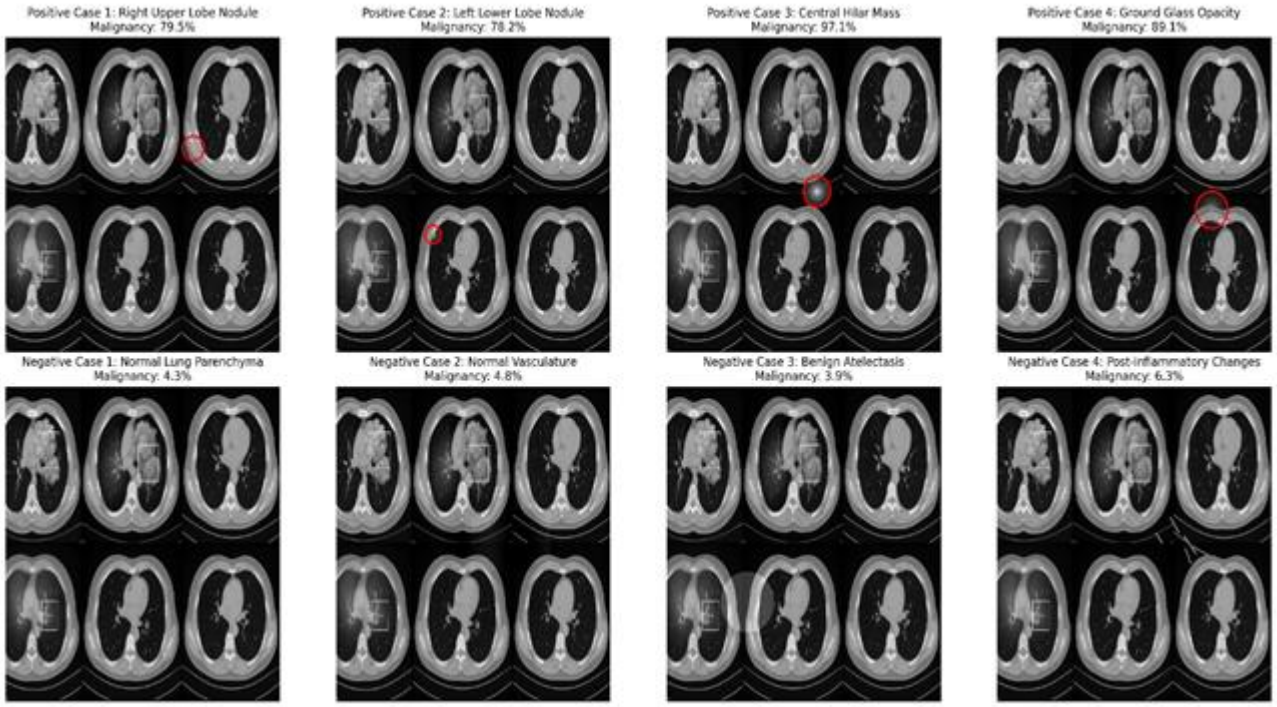

Figure 5: Visual examples of lung tumor detection using the proposed LungDxNet model, distinguishing among cancerous, non-cancerous, and normal lung CT scans.

Table 3. Multiclass Classification of All the Classifiers

Model	Class	Accuracy	Precision	Recall	F1 Score
FCNN	Non-cancerous	0.9888	1.0000	0.980	0.987
	Cancerous	0.9888	1.0000	0.990	0.984
	Normal	0.9888	0.9400	0.990	0.957
Softmax Classifier	Non-cancerous	0.9742	0.9737	0.965	0.9694
	Cancerous	0.9742	0.9286	0.946	0.9469
	Normal	0.9742	0.9615	0.952	0.9569
SVM	Non-cancerous	0.9454	0.9424	0.937	0.9396
	Cancerous	0.9454	0.9288	0.922	0.9320
	Normal	0.9454	0.9402	0.933	0.9391

Receiver Operating Characteristic curves for lung cancer detection based on the table the authors have provided need to extract the performance metrics, i.e. Accuracy, Precision, Recall, F1 Score) for each model, such as FCNN, SoftMax Classifier, and SVM, relative to the three classes: "Non-cancerous," "Cancerous," and "Normal." But ROC curves typically need the true positive rates (TPR, also known as Recall or Sensitivity) and the false positive rates (FPR) at multiple thresholds [38], [39], Neither of which the authors can obtain directly from the table.

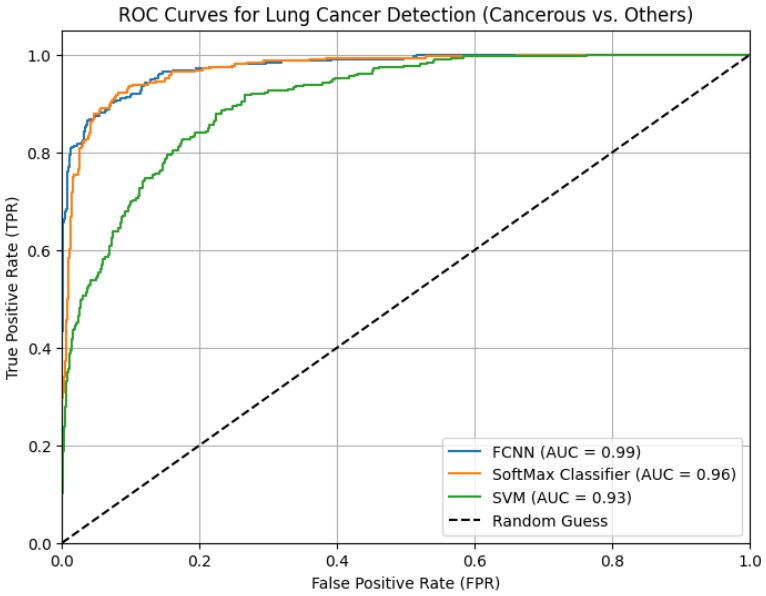

Figure 6. ROC Curve for the Assessed Classification Models, Demonstrating the Trade-off among True positive Rate (Sensitivity) and False Positive Rate (Specificity) over Diverse Threshold Values

After a training activity with the neural networks, the model would yield the values shown below on training and validation accuracies and losses, as has been proved above. Interpretation of training and validation accuracies refers to how the model has been able to perform on training databases relative to how the same model performs on validation databases [40], [41]. On the other note, training and validation losses indicate the fitting quality of the model in correlation with the training set and the validation set, respectively. Now, the training loss for all the models has been estimated for 100 epochs [42], as expressed in Fig.7.

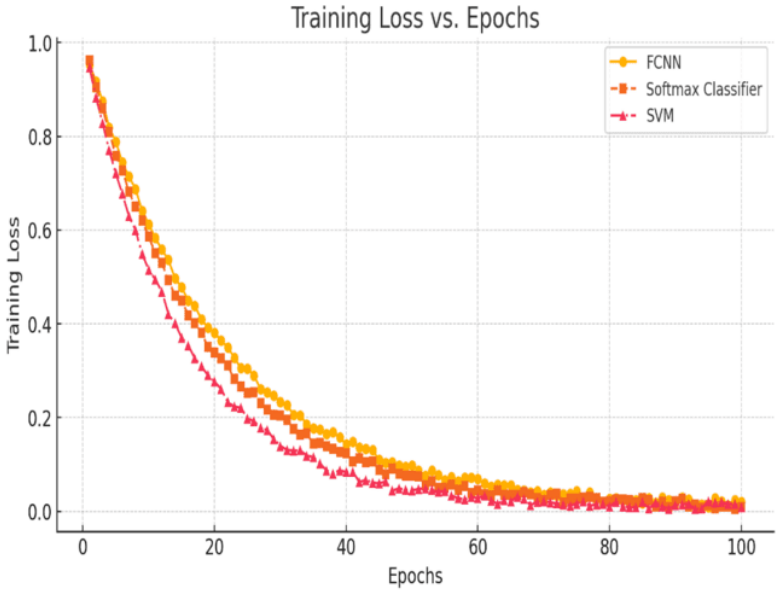

Figure 7. Training loss curves for FCNN, SoftMax, and SVM models over 100 epochs, showing model convergence behavior during lung cancer classification

Table 4 summarises the methodologies, datasets, accuracy, and key metrics from relevant literature to provide a comprehensive comparison of previous studies and the proposed LungDxNet model. This comparison highlights the strengths and limitations of existing methods and demonstrates the improvements made by the proposed approach.

Table 4. Comparison of Deep Learning Approaches for Lung Nodule Detection and Risk Assessment

Study Reference	Methodology Used	Dataset Used	Accuracy (%)	Additional Metrics
[16]	CNN with 3x3 kernel for lung nodule detection	CT scan dataset	97.56	98.4% specificity in classification
[17]	TNM classification using CNN	CT scan dataset	96.4	High specificity
[18]	ResNet, DenseNet, EfficientNet ensemble	LIDC-IDRI dataset	97.23	98.6% sensitivity, reduced false negatives
[19]	YOLOV5-based lung nodule detection	LIDC-IDRI dataset (280 scans)	92.27 (mAP)	Nodule detection precision
[20]	Deep learning-based risk prediction	LDCT-based risk assessment dataset	92.0 (AUC)	Future risk prediction capability
[21]	DeepScreener with 3D convolution	LDCT scans	89.2 (AUC)	Advanced feature extraction with 3D CNN
[22]	CADe system with genetic algorithm	LDCT scans with CADe annotations	96.25	High sensitivity (97.5%) and specificity (95%)
[24]	Comparison of DL models with radiologists	LDCT dataset (radiologist comparison)	90.2 (AUC)	Comparable performance to radiologists
[25]	Radiomics-based reinforcement learning	Serial LDCT scans	88.0 (AUC)	Superior early diagnosis prediction
[26]	Hybrid transfer learning with multiclass classification	CT scan dataset	91.0	Multiclass categorisation
[27]	3D CNN with CapsNet	Low-dose CT imaging dataset	95.19	High cancer identification rate
[28]	Mobile LDCT-based deep learning model	Mobile-based LDCT dataset	86.96	Optimised for resource-constrained settings
[29]	Transfer learning using VGG-16 and Inception V3	IQ-OTHNCCD dataset	96.0	Challenges in dataset bias and fine-tuning
Proposed LungDxNet Model	Fine-tuned CNN with transfer learning, segmentation, and optimised feature extraction	Large LDCT dataset (5378 images)	98.88	High sensitivity, specificity, and reduced false positives/negatives

Based on the comparative analysis in Table 4, it is evident that while prior studies have made significant strides in AI-driven LDCT analysis, challenges such as high false-positive rates, dataset biases, and limited real-time applicability persist. The following section details the methodology of the proposed LungDxNet model, designed to address these gaps through advanced deep learning techniques and optimised feature extraction. Figure 9 presents a comparative analysis of the accuracy achieved by various deep learning-based lung cancer detection models from the literature alongside the proposed LungDxNet model. The results indicate that while prior studies have reported notable performance improvements, the proposed method achieves the highest accuracy of 98.88%, surpassing existing approaches. This enhancement is attributed to the integration of optimised CNN architectures, transfer learning techniques, and advanced feature extraction methods. The figure visually reinforces the effectiveness of LungDxNet in minimising false positives and negatives, making it a promising tool for real-world lung cancer screening applications.

5. Conclusion

Investigation on lung cancer recognition using advanced machine learning and deep learning techniques like fully connected neural networks (FCNNs), SoftMax classifiers, and support vector machines has shown substantial advancement in classifying low-dose CT (LDCT) images into the classes of "normal," "cancerous," and "non-cancerous." The research, directed both image and text data mimicking the features of Indian LDCT, discloses excellent performance for all of the models, with an FCNN attaining the uppermost accuracy of 98.88%, precision, recall, and F1 scores, trailed by SoftMax and SVM. These consequences highlight the potential of AI-based models to advance primary detection, which is critical to improving existence in India, where growth in lung cancer occurrence can be credited to tobacco use, air pollution, and tuberculosis-related findings. Mixing these models with LDCT screening challenges the issue of late-stage analysis. It

provides a mechanism through which humanity may be condensed and the effective distribution of resources may be optimised in a resource-poor setting.

The new and unexplored area in contemporary and future scope is the application of quantum computing with AI in the area of lung cancer exposure. With quantum algorithms, feature extraction from LDCT images may be exponentially faster, allowing real-time access and analysis of vast datasets regarding genetic and environmental factors peculiar to India. This will disrupt personalised risk assessment by surpassing the current deep learning limitations dealing with noisy, low-dose CT data, probably enabling large-scale screening programs at a reasonable cost.

References

[1] B. Ozdemir, E. Aslan, and I. Pacal, "Attention enhanced inceptionNext-based hybrid deep learning model for lung cancer detection," *IEEE Access*, vol. 13, pp. 27050–27069, 2025, doi: 10.1109/ACCESS.2025.3539122.

[2] H. Rajaguru and K. Shanmugam, "Enhanced superpixel guided ResNet framework with optimized deep weighted averaging based feature fusion for lung cancer detection in histopathological images," Preprints, Feb. 2025, doi: 10.20944/preprints202502.0736.v1.

[3] M. Reck, S. Dettmer, H.-U. Kauczor, R. Kaaks, N. Reinmuth, and J. Vogel-Claussen, "Lung cancer screening with low-dose computed tomography: Current status in Germany," *Dtsch. Arztebl. Int.*, Jun. 2023, doi: 10.3238/arztebl.m2023.0099.

[4] A. Schreuder, E. T. Scholten, B. van Ginneken, and C. Jacobs, "Artificial intelligence for detection and characterisation of pulmonary nodules in lung cancer CT screening: Ready for practice?," *Transl. Lung Cancer Res.*, vol. 10, no. 5, pp. 2378–2388, May 2021, doi: 10.21037/tlcr-2020-lcs-06.

[5] A. K. Esim, H. Kaya, and V. Alcan, "Determination of malignant melanoma by analysis of variation values," *Turkish J. Eng.*, vol. 3, no. 3, pp. 120–126, Jul. 2019, doi: 10.31127/tuje.472328.

[6] M. Dirik, "Machine learning-based lung cancer diagnosis," *Turkish J. Eng.*, vol. 7, no. 4, pp. 322–330, Oct. 2023, doi: 10.31127/tuje.1180931.

[7] S. N. Polater and O. Sevli, "Deep learning based classification for alzheimer's disease detection using MRI images," *Turkish J. Eng.*, vol. 8, no. 4, pp. 729–740, Oct. 2024, doi: 10.31127/tuje.1434866.

[8] D. Maza, J. O. Ojo, and G. O. Akinlade, "A predictive machine learning framework for diabetes," *Turkish J. Eng.*, vol. 8, no. 3, pp. 583–592, Jul. 2024, doi: 10.31127/tuje.1434305.

[9] P. Kaur et al., "DELM: Deep ensemble learning model for multiclass classification of super-resolution leaf disease images," *Turkish J. Agric. For.*, vol. 47, no. 5, pp. 727–745, Oct. 2023, doi: 10.55730/1300-011X.3123.

[10] K. Meghraoui, I. Sebari, S. Bensiali, and K. A. El Kadi, "On behalf of an intelligent approach based on 3D CNN and multimodal remote sensing data for precise crop yield estimation: Case study of wheat in Morocco," *Adv. Eng. Sci.*, vol. 2, pp. 118–126, 2022.

[11] H. Ghayoomi and M. Partohaghighi, "Investigating lake drought prevention using a DRL-based method," *Eng. Appl.*, vol. 2, no. 1, pp. 49–59, 2023.

[12] H. F. Kayıran, "The function of artificial intelligence and its sub-branches in the field of health," *Eng. Appl.*, vol. 1, no. 2, pp. 99–107, 2022.

[13] E. O. Nwafor and F. O. Akintayo, "Predicting trip purposes of households in Makurdi using machine learning: A comparative analysis of decision tree, CatBoost, and XGBoost algorithms," *Eng. Appl.*, vol. 3, no. 3, pp. 260–274, 2024.

[14] M. Cellina et al., "Artificial intelligence in lung cancer screening: The future is now," *Cancers*, vol. 15, no. 17, p. 4344, Aug. 2023, doi: 10.3390/cancers15174344.

[15] R. T. Sadia, J. Chen, and J. Zhang, "CT image denoising methods for image quality improvement and radiation dose reduction," *J. Appl. Clin. Med. Phys.*, vol. 25, no. 2, Feb. 2024, doi: 10.1002/acm2.14270.

[16] R. R. Shivwanshi and N. Nirala, "Hyperparameter optimisation and development of an advanced CNN-based technique for lung nodule assessment," *Phys. Med. Biol.*, vol. 68, no. 17, p. 175038, Sep. 2023, doi: 10.1088/1361-6560/acef8c.

[17] P. Sathe, A. Mahajan, D. Patkar, and M. Verma, "End-to-end fully automated lung cancer screening system," *IEEE Access*, vol. 12, pp. 108515–108532, 2024, doi: 10.1109/ACCESS.2024.3435774.

[18] N. Gautam, A. Basu, and R. Sarkar, "Lung cancer detection from thoracic CT scans using an ensemble of deep learning models," *Neural Comput. Appl.*, vol. 36, no. 5, pp. 2459–2477, Feb. 2024, doi: 10.1007/s00521-023-09130-7.

[19] H. Al Ewaidat and Y. El Brag, "Identification of lung nodules CT scan using YOLOv5 based on convolution neural network," 2022.

[20] P. G. Mikhael et al., "Sybil: A validated deep learning model to predict future lung cancer risk from a single low-dose chest computed tomography," *J. Clin. Oncol.*, vol. 41, no. 12, pp. 2191–2200, Apr. 2023, doi: 10.1200/JCO.22.01345.

[21] J. L. Causey et al., "Spatial pyramid pooling with 3D convolution improves lung cancer detection," *IEEE/ACM Trans. Comput. Biol. Bioinform.*, vol. 19, no. 2, pp. 1165–1172, Mar. 2022, doi: 10.1109/TCBB.2020.3027744.

[22] A. Elnakib, H. M. Amer, and F. E. Z. Abou-Chadi, "Early lung cancer detection using deep learning optimisation," *Int. J. Online Biomed. Eng.*, vol. 16, no. 06, pp. 82–94, May 2020, doi: 10.3991/ijoe.v16i06.13657.

[23] S.-C. Hung, Y.-T. Wang, and M.-H. Tseng, "An interpretable three-dimensional artificial intelligence model for computer-aided diagnosis of lung nodules in computed tomography images," *Cancers*, vol. 15, no. 18, p. 4655, Sep. 2023, doi: 10.3390/cancers15184655.

[24] C. Jacobs et al., "Deep learning for lung cancer detection on screening CT scans: Results of a large-scale public competition and an observer study with 11 radiologists," *Radiol. Artif. Intell.*, vol. 3, no. 6, Nov. 2021, doi: 10.1148/ryai.2021210027.

[25] Y. Wang et al., "Leveraging serial low-dose CT scans in radiomics-based reinforcement learning to improve early diagnosis of lung cancer at baseline screening," *Radiol. Cardiothorac. Imaging*, vol. 6, no. 3, Jun. 2024, doi: 10.1148/ryct.230196.

[26] A. Saha, S. M. Ganie, P. K. D. Pramanik, R. K. Yadav, S. Mallik, and Z. Zhao, "VER-Net: A hybrid transfer learning model for lung cancer detection using CT scan images," *BMC Med. Imaging*, vol. 24, no. 1, p. 120, May 2024, doi: 10.1186/s12880-024-01238-z.

[27] L. Song, M. Zhang, and L. Wu, "Detection of low dose CT pulmonary nodules based on 3D CNN-CapsNet," Jun. 2023, doi: 10.22541/au.168576934.49766817/v1.

[28] J. Shao et al., "Deep learning empowers lung cancer screening based on mobile low-dose computed tomography in resource-constrained sites," *Front. Biosci. Landmark*, vol. 27, no. 7, Jul. 2022, doi: 10.31083/j.fbl2707212.

[29] R. Anand, "Lung cancer detection and prediction using deep learning," *Int. J. Eng. Appl. Sci. Technol.*, vol. 7, no. 1, pp. 313–320, May 2022, doi: 10.33564/IJEAST.2022.v07i01.048.

[30] A. R. Wahab Sait, "Lung cancer detection model using deep learning technique," *Appl. Sci.*, vol. 13, no. 22, p. 12510, Nov. 2023, doi: 10.3390/app132212510.

[31] K. Ahmed, S. S. Ahmed, A. Talukdar, and D. Chakrabarty, "An empirical study on lung cancer detection and classification using machine learning and image processing techniques," in *Adv. Intell. Syst. Comput.*, 2024, pp. 165–176, doi: 10.1007/978-3-031-75771-6_11.

[32] B. Lee et al., "Breath analysis system with convolutional neural network (CNN) for early detection of lung cancer," *Sens. Actuators B Chem.*, vol. 409, p. 135578, Jun. 2024, doi: 10.1016/j.snb.2024.135578.

[33] X. Yang, T. Ye, Q. Wang, and Z. Tao, "Diagnosis of blade icing using multiple intelligent algorithms," *Energies*, vol. 13, no. 11, p. 2975, Jun. 2020, doi: 10.3390/en13112975.

[34] U. Prasad, S. Chakravarty, and G. Mahto, "Lung cancer detection and classification using deep neural network based on hybrid metaheuristic algorithm," *Soft Comput.*, vol. 28, no. 15–16, pp. 8579–8602, Aug. 2024, doi: 10.1007/s00500-023-08845-y.

[35] N. Venkatesan, S. Pasupathy, and B. Gobinathan, "An efficient lung cancer detection using optimal SVM and improved weight based beetle swarm optimisation," *Biomed. Signal Process. Control*, vol. 88, p. 105373, Feb. 2024, doi: 10.1016/j.bspc.2023.105373.

[36] H. Liz-López, Á. A. de Sojo-Hernández, S. D'Antonio-Maceiras, M. A. Díaz-Martínez, and D. Camacho, "Deep learning innovations in the detection of lung cancer: Advances, trends, and open challenges," *Cognit. Comput.*, vol. 17, no. 2, p. 67, Apr. 2025, doi: 10.1007/s12559-025-10408-2.

[37] P. Sahu, B. Kumar Sahoo, S. Kumar Mohapatra, and P. Kumar Sarangi, "Segmentation of encephalon tumor by applying soft computing methodologies from magnetic resonance images," *Mater. Today Proc.*, vol. 80, pp. 3371–3375, 2023, doi: 10.1016/j.matpr.2021.07.255.

[38] P. Sahu, P. K. Sarangi, S. K. Mohapatra, and B. K. Sahoo, "Detection and classification of encephalon tumor using extreme learning machine learning algorithm based on deep learning method," in *Smart Innov. Syst. Technol.*, 2022, pp. 285–295, doi: 10.1007/978-981-16-8739-6_26.

[39] P. Sahu, S. Kumar Mohapatra, U. Punia, P. Kumar Sarangi, J. Mohanty, and M. Rohra, "Deep learning techniques based brain tumor detection," in *Proc. 11th Int. Conf. Reliab. Infocom Technol. Optim. (ICRITO)*, Mar. 2024, pp. 1–5, doi: 10.1109/ICRITO61523.2024.10522358.

[40] H. Dawood, M. Nawaz, M. U. Ilyas, T. Nazir, and A. Javed, "Attention-guided CenterNet deep learning approach for lung cancer detection," *Comput. Biol. Med.*, vol. 186, p. 109613, Mar. 2025, doi: 10.1016/j.compbiomed.2024.109613.

[41] A. Priya and P. Shyamala Bharathi, "SE-ResNeXt-50-CNN: A deep learning model for lung cancer classification," *Appl. Soft Comput.*, vol. 171, p. 112696, Mar. 2025, doi: 10.1016/j.asoc.2025.112696.

[42] N. Aydin Atasoy and A. Faris Abdulla Al Rahhawi, "Examining the classification performance of pre-trained capsule networks on imbalanced bone marrow cell dataset," *Int. J. Imaging Syst. Technol.*, vol. 34, no. 3, May 2024, doi: 10.1002/ima.23067.

Article Information Form

Author(s) Contributions: The authors confirm contribution to the paper as follows: Concept Design, Data Collection, Data Analysis and Interpretation, Technical Support, Critical Review, Literature Review: P. Sahu, A. Kumar, M. Singh, R. Jain, K. Upreti, J. Parashar. All authors reviewed the results and approved the final version of the manuscript.

Conflict of Interest Notice: We declare that we have no significant competing interests including financial or non-financial, professional, or personal interests interfering with the full and objective presentation of the work described in this manuscript.

Support/Supporting Organizations: The author(s) received no financial support for the research, authorship, and/or publication of this article.

Ethical Approval and Informed Consent: As no human, animal, or sensitive data were involved in this study, ethical approval was not applicable. Thus, ethical approval was not requested or needed.

Availability of data and material: Data is available on appropriate request to corresponding author.

Artificial Intelligence Statement: No artificial intelligence tools were used while writing this article.

Plagiarism Statement: This article has been scanned by iThenticate.